Weak line water vapor spectrum in the 11,787 – 13,554 cm^{-1} region

Roman N. Tolchenov, Jonathan Tennyson

Department of Physics and Astronomy, University College London, Gower Street, London WC1E 6BT, U.K.

J. W. Brault and A.A.D. Canas,

LASP (Space Technology Building), 1234 Innovation Drive, Boulder, CO 80303-7814 U.S.A.

Roland Schermaul

Laser Optics & Spectroscopy, Blackett Laboratory, Imperial College of Science, Technology and Medicine, Prince Consort Road, London SW7 2BW, U.K.

Abstract

Long pathlength Fourier Transform spectra of water vapor recorded previously by Schermaul *et al*, (J. Molec. Spectrosc. **211**, 169 (2002)) are analysed in the range 11,787 – 13,554 cm^{-1}. Wavenumbers, absolute intensities and self-broadening coefficients, with associated uncertainties, are presented for 2137 lines. Analysis of these lines using variational linelists has been conducted leading to the assignment of 1906 of the new lines to 23 different upper vibrational states in the $3\nu + \delta$, 4ν and $4\nu + \delta$ polyads, a further 19 lines are ascribed to $H_2{}^{18}O$. Comparisons are made with the HITRAN database.

Key words: water vapor; near-infrared and visible spectrum; line assignments;line intensities; self-broadening coefficients

Email address: roman@theory.phys.ucl.ac.uk and j.tennyson@ucl.ac.uk (Roman N. Tolchenov, Jonathan Tennyson).

1 Introduction

Combined experimental and theoretical studies [1] have suggested that there are problems with the near-infrared spectroscopic water vapor data used in previous versions of the HITRAN database [2]. This finding is of particular significance because of the serious discrepancy between the observed and the modelled values of the atmospheric radiation budget [3,4]. As part of a concerted attempt to resolve problems with water vapor spectra, Schermaul *et al* [5–7] recorded a series of long pathlength spectra water vapor spectra at near infrared and optical wavelengths. In particular they recorded spectra of pure water vapor in the 6,500 – 16,400 cm^{-1} range which, for most of this range, probed significantly deeper than previous studies. The objective of this work was not the re-determination of the line parameters of the stronger lines but the detection and characterization of the many very weak transitions also present in the spectrum. In their paper reporting these spectra [7], Schermaul *et al* only analysed one portion of their results covering the 13,200 – 15,000 cm^{-1} region. By using the results of variational nuclear motion calculations [8,9] they were able to make 952 new line assignments covering 35 different vibrational states of $H_2{}^{16}O$.

In fact, comparison of the signal-to-noise ratio in the pure water vapor spectra of Schermaul *et al* [7] suggests that the biggest improvement compared to previous studies is not for their spectrum 4, spanning 13,200 – 15,000 cm^{-1}, which they analysed but for their spectrum 3. This spectrum covers the frequency range 11,780–14,500 cm^{-1} and its analysis is the subject of this paper.

The 11,780–14500 cm^{-1} spectrum of Schermaul *et al* contains 2137 lines below 13,554 cm^{-1}. This is significantly more than the previous works in this region [10–12]. Toth [10] and Flaud *et al* [11] covered a similar, smaller region between 11600 and 12750 cm^{-1}. These studies contained 930 and 917 lines respectively compared to 1524 lines reported here for the same region. While Flaud *et al* assigned all except 9 of their lines, Toth assigned 785 of his lines. Only Toth's assigned lines appear to be included in the latest edition of HITRAN [2]. HITRAN does contain further lines in this region but their source is unclear to us. At the higher frequencies here HITRAN also contains data due to Mandin *et al* [13], which have also been the subject of more recent analysis [7,14,15]. The most recent HITRAN contains a total of 1566 $H_2{}^{16}O$ lines in the 11,787 – 13,554 cm^{-1} region of this work compared to the 2137 lines presented here. Comparison with the results presented in HITRAN and the previous assignments are made below.

2 Experimental data

The experimental procedure used by Schermaul *et al* [7] to obtain their water vapor spectra is discussed in considerable detail in their original work. Their spectrum number 3 covered the wavenumber range 11,780–14,500 cm^{-1} using 926 scans, a pathlength of 800.8 $\pm$1.0 m and a vapor pressure of 21.15 $\pm$0.08 hPa at a temperature of 296.0 $\pm$0.7 K. The estimated signal-to-noise ratio was 1200:1, a significant improvement on Flaud *et al* [11,12] which appears to be the best available in the literature.

Line parameters of the individual transitions were determined from the absorbance spectra using an interactive least-squares line-fitting procedure that is part of the GREMLIN spectrum analysis software (Brault, unpublished). The general aim was to fit Voigt line profiles to all lines, such that the residuals of the fit were indistinguishable from the noise. This was usually possible, except when a line was so strong that the peak absorbance approached saturation, and when the wavenumber separation of a pair of lines was so small that the least-squares routine could not find a stable two-line solution. Saturation was a common problem and simultaneous fitting of up to several tens of lines was often necessary. Interactive use of GREMLIN allowed weak line parameters to be determined even when they are blended with strong (saturated) lines by a variety of techniques including manually removing the central portion of the strong line(s) from the fit. Parameters for the strong lines are much better determined using studies with shorter pathlengths [5].

The molecular line-shape was assumed to be a Voigt line profile, i.e., a convolution of Lorentzian (pressure-broadened) and Gaussian (Doppler-broadened) contributions. Although the Doppler contribution to a Voigt profile caused by the motion of the particles can generally be calculated and only the Lorentzian needs to be fitted, the effect of collisional narrowing can be strong enough to seriously distort standard Voigt line profiles, see [16]. As in the previous work by Schermaul *et al* [7], 'generalized' Voigt profiles, profiles for which both Lorentzian and Gaussian contributions are adjusted, were employed. No allowance was made for pressure induced shifts in the frequencies. A total of 2137 lines were characterised up to 13,554 cm^{-1}; above this wavenumber the previously analysed 13,200 – 15,000 cm^{-1} spectrum of Schermaul *et al* [7] has better signal-to-noise.

The output of the fitting procedure allowed us to obtain values of the line position, the intergrated absorption intensity at 296 K and the self-broadening parameter; in each case with associated statistical errors. It should be noted that for strong lines, characterized by having an intensity greater than 5×10^{-24} cm $molecule^{-1}$, see below, saturation effects means that there are much larger systematic errors associated with the line parameters than the tabulated sta-

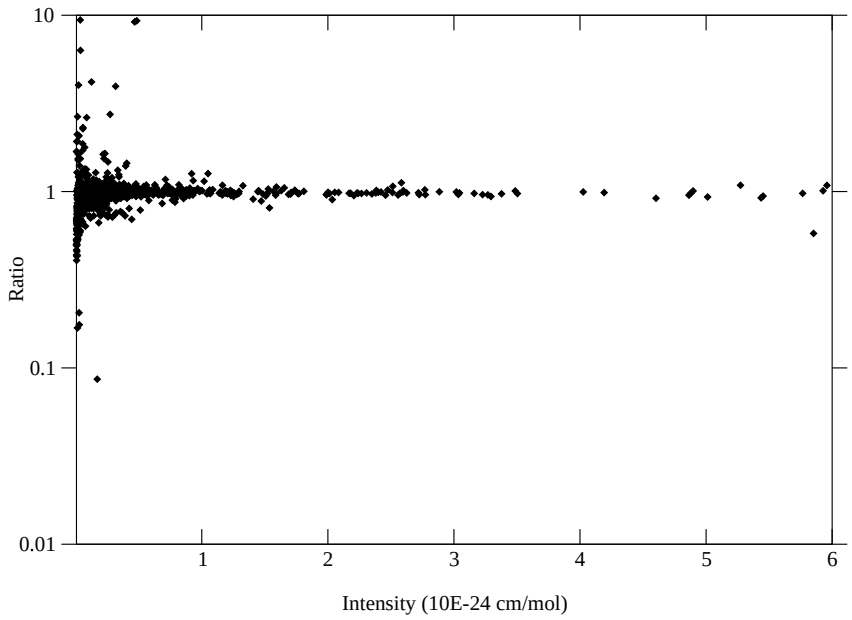

Fig. 1. Comparison of intensities measured in this work with those given in the 2000 edition of HITRAN [2] in the frequency range 11,787 – 13,554 cm^{-1}. Given is the ratio of I(this work) to I(HITRAN) as a function of the intensity measured here.

tistical errors. Data on these lines is more reliably obtained from less sensitive previous studies. In particularly Schermaul *et al* [5] recorded shorter path-length water-air spectra in this frequency range specifically with the aim of obtaining reliable intensity information for these strong lines. A full list of fitted lines is given in the journal's electronic archive. This list includes uncertainties for each parameter (wavenumber, intensity, self-broadening) listed. These uncertainties are purely the statistical ones determined by the fit. In practice a minimum error of 0.001 cm^{-1} was imposed on the transition wavenumber when determining the energy levels to allow for pressure shifts and other systematic errors.

Even without spectroscopic assignment it is possible to make comparison with some of the data given in HITRAN [2]. Figure 1 compares intensities fitted during the present work with those given in HITRAN. Only lines weaker than 5.5×10^{-24} cm $molecule^{-1}$ are compared since lines stonger than this show systematic errors in our work which make them appear weaker than they should be. There is good agreement between our data and the corrected HITRAN for lines in the intensity range $1-5.5\times10^{-24}$ cm $molecule^{-1}$, although there is a systematic increase in the disagreement as the lines get weaker. We believe that this increased scatter in the weaker lines is a reflection of the

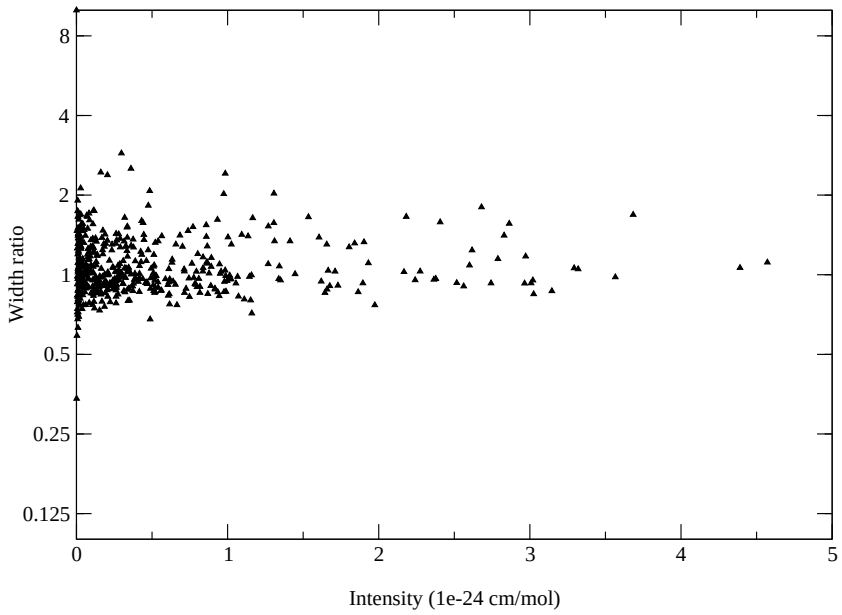

Fig. 2. Comparison of self-broadening coefficients, $\gamma_L(H_2O)$, measured in this work with those given in HITRAN [2] in the frequency range 11,787 – 13,554 cm^{-1}. Given is the ratio of $\gamma_L(H_2O)$(this work) to $\gamma_L(H_2O)$(HITRAN) as a function of the line intensity measured here.

large statistical errors in the data reported in HITRAN for these lines. Our new parameters for these lines should be considerably more accurate than those determined previously.

There is an apparent inconsistency between the finding of Belmiloud *et al* [1] that HITRAN systematically underestimates the strength of water lines in the near-infrared and our finding of good agreement between the two sets of intensity data. However these studies are not equivalent: Belmiloud *et al* analysis was primarily concerned with the intensity of the very important strong absorption features; our work here is only reliable for the many weak absorption features. In practice the water-air data [5,6] analysed by Belmiloud *et al* is only sensitive to strong absorptions which are saturated in the present pure water vapor study. Thus the line parameters extracted from this study essentially have no overlap with those given there despite covering the same spectral region.

Figure 2 compares self-broadening coefficients fitted here with those given by HITRAN [2]. The data is again arranged by intensity of the line and lines with intensity greater than 5×10^{-24} cm $molecule^{-1}$ are omitted from the

comparison. For lines intensities in the range $1.5 - 5 \times 10^{-24}$, there is again fair agreement between the line parameters determined here and those presented by HITRAN. For weaker lines we believe our data to be more reliable.

3 Line assignments

Initial assignments were made using known energy levels taken from the recent tabulation of Tennyson *et al* [17]. Many lines could be assigned this way including, of course, lines assigned in previous studies of this region. These assignments are designated 'trivial'. The remaining unassigned lines were analysed by a variety of techniques.

Tanaka *et al* [18] have recently analysed $H_2{}^{18}O$ enriched spectra in the region we consider here. Comparison with this work identified 19 transitions as belonging to $H_2{}^{18}O$. These have been so labelled in the electronic listing of the data but a more thorough analysis is left to Tanaka *et al.*

Assignments to transitions involving previously unobserved levels in $H_2{}^{16}O$ were made by searching for possible combination differences and by comparison with the variational linelist of Partridge and Schwenke [8].

As a result of this analysis 1906 transitions could be assigned to transitions involving $H_2{}^{16}O$. These transitions involved 23 vibrational states largely in the $3\nu + \delta$ and 4ν polyads. Some transitions to states in the $4\nu + \delta$ polyad were also observed, arising mainly from hot bands. Table 1 summarizes our results in terms of trivial and new assignments. All assignments are given in the electronic archive.

Since HITRAN contains a considerable number of lines in the region considered here it is interesting to compare our assignments with those given there. We found a considerable level of disagreement. Table 2 lists HITRAN transitions which we have re-assigned. Not included in Table 2 are transitions given in HITRAN as involving the (202) state but which, following Carleer *et al* [15], should be relabelled as belong to (400). Table 3 lists new assignments to lines tabulated in HITRAN without assignments. Finally in the electronic archive we give a listing of 251 lines for which the assignments given in HITRAN for the 11,787 – 13,554 cm^{-1} region appear to be wrong. Many of these lines have already been identified as misassigned in previous studies [8,14,19].

Comparison of our line assignments with those of Flaud *et al* [11], who give 917 lines between 11,600 and 12,750 cm^{-1} are much closer. We found it necessary to reassign only 2 of their lines and were able to assign 4 of their 9 unassigned lines.

One result of the present study is the assignment of transitions to previously unobserved energy levels in water. These transitions have been used to augment the energy level compilation of Tennyson *et al* [17]. As a result of this work 199 new levels have been determined spread across a total of 14 different vibrational states, although it should be noted that many of these new levels have not been confirmed by combination differences. Updated energy levels can be found at ftp.tampa.phys.ucl.ac.uk/pub/astrodata/water/levels. Energy levels, including statistical errors, are given for the states (230), (131), (032) (310), (211), (112), (013) and (141) in the electronic archive.

4 Conclusions

A previously recorded long-path length Fourier transform spectrum of water vapor for the region 11,787 – 13,554 cm^{-1} has been analysed. This spectrum has a better signal-to-noise ratio than previous studies of this region. Besides characterizing more lines than the comparable studies, the spectrum should also provide more reliable absorption parameters for weak water lines, those with intensity less than 5×10^{-24} cm $molecule^{-1}$, in this spectral region. The importance of precisely characterizing the absorption by water vapor at near-infrared and optical wavelengths has recently been re-emphasized by the atmospheric models focusing on the role weak water lines [20,21]. The present study provides not only improved laboratory data towards this goal but also data to improve theoretical models which might ultimately provide a complete solution of this difficult but important problem.

Acknowledgements

We acknowledge the contributation of our late friend and colleague Richard Learner to this work. We thank Nikolai Zobov and Oleg Polyansky for helpful discussions. This work was supported by the UK Natural Environment Research Council under Grants GR3/11097, GR3/11674 and NER/A/S/2000/01315.

References

[1] D. Belmiloud, R. Schermaul, K. Smith, N. F. Zobov, J. Brault, R. C. M. Learner, D. A. Newnham and J. Tennyson, *Geophys. Res. Lett.*, **27**, 3703-3706 (2000).

[2] L. S. Rothman, C. P. Rinsland, A. Goldman, S. T. Massie, D. P. Edwards, J.-M. Flaud, A. Perrin, C. Camy-Peyret, V. Dana, J.-Y. Mandin, J. Schroeder,

A. McCann, R. R. Gamache, R. B. Wattson, K. Yoshino, K. V. Chance, K. W. Jucks, L. R. Brown, V. Nemtchinov and P. Varanasi, *J. Quant. Spectrosc. Radiat. Transfer* **60**, 665-710 (1998); for HITRAN2000 see www.hitran.com.

[3] A. Arking, *J. Climate* **12**, 1589-1600, 1999.

[4] V. Ramanathan and A. M. Vogelmann, *Ambio*, **26**, 38-46 (1997).

[5] R. Schermaul, R. C. M. Learner, D. A. Newnham, R. .G. Williams, J. Ballard, N. F. Zobov, D. Belmiloud and J. Tennyson, *J. Molec. Spectrosc.*, **208**, 32-42 (2001).

[6] R. Schermaul, R. C. M. Learner, D. A. Newnham, J. Ballard, N. F. Zobov, D. Belmiloud and J. Tennyson, *J. Molec. Spectrosc.*, **208**, 43-50 (2001).

[7] R. Schermaul, R. C. M. Learner, A. A. D. Canas, J. W. Brault, O. L. Polyansky, D. Belmiloud and J. Tennyson, *J. Molec. Spectrosc.*, **211**, 169-178 (2002).

[8] H. Partridge and D. W. Schwenke, *J. Chem. Phys.* **106**, 4618-4639 (1997).

[9] O.L. Polyansky, J. Tennyson, and N.F. Zobov, N.F. 1999 *Spectrochemica Acta*, **55A**, 659 (1999).

[10] R. A. Toth, *J. Mol. Spectrosc.* **166**, 176-183 (1994).

[11] J.-M. Flaud, C. Camy-Peyret, A. Bykov, O. Naumenko, T. Petrova, A. Scherbakov, and L. Sinitsa, *J. Mol. Spectrosc.* **183**, 300-309 (1997).

[12] J.-M. Flaud, C. Camy-Peyret, A. Bykov, O. Naumenko, T. Petrova, A. Scherbakov, and L. Sinitsa, *J. Mol. Spectrosc.* **185**, 211-221 (1997).

[13] J.-Y. Mandin, J.-P. Chevillard, C. Camy-Peyret and J.-M. Flaud, *J. Mol. Spectrosc.* **116**, 167-190 (1986).

[14] O. L. Polyansky, N. F. Zobov, S. Viti and J. Tennyson, *J. Mol. Spectrosc.* **189**, 291-300 (1998).

[15] M. Carleer, A. Jenouvrier, A.-C. Vandaele, P. F. Bernath, M. F. Mérienne, R. Colin, N. F. Zobov, O. L. Polyansky, J. Tennyson and A. V. Savin, *J. Chem. Phys.* **111**, 2444-2450 (1999)

[16] R. Schermaul and , R. C. M. Learner, *J. Quant. Spectrosc. Radiat. Transfer* **61**, 781-794 (1999).

[17] J. Tennyson, N. F. Zobov, R. Williamson, O. L. Polyansky and P. F. Bernath, *J. Phys. Chem. Ref. Data*, **30**, 735-831 (2001).

[18] M. Tanaka, J. W. Brault and J. Tennyson, *J. Mol. Spectrosc.*, (submitted).

[19] D. W. Schwenke, *J. Mol. Spectrosc.*, **190**, 397-402 (1998).

[20] R. C. M. Learner, W. Zhong, J. D. Haigh, D. Belmiloud and J. Clarke, *Geophys. Res. Lett.* **26**, 3609-3612 (1999).

[21] W. Zhong, J. D. Haigh, D. Belmiloud, R. Schermaul and J. Tennyson, *Quart. J. Roy. Metr. Soc.* **127**, 1 615-1626 (2001).

Table 1
Summary of $H_2{}^{16}O$ transitions assigned in the 11,800 – 14,500 cm^{-1} region

Band		ω [17]	lines	
local mode	normal mode	(cm^{-1})	a	b
$(1,0)^-5$	051		2	6
$(2,0)^+3$	230	11767.390	43	27
$(2,0)^-3$	131	11813.207	158	14
(1,1) 3	032	12007.776	54	26
$(3,0)^+1$	310	12139.315	126	30
$(3,0)^-1$	211	12151.254	376	25
$(2,1)^+1$	112	12407.662	246	23
$(2,1)^-1$	013	12565.007	267	24
(0,0) 8	080		1	0
$(1,0)^+6$	160		2	8
$(1,0)^-6$	061		5	9
$(2,0)^+4$	240		27	7
$(2,0)^-4$	141	13256.000	48	19
(1,1) 4	042	13453.000	17	0
$(3,0)^+2$	320		47	1
$(3,0)^-2$	221	13652.656	116	1
$(4,0)^+0$	400	13828.277	49	0
$(4,0)^-0$	301	13830.938	77	0
$(1,0)^-7$	071	13835.372	2	0
$(2,1)^+2$	122	13910.896	3	0
$(2,1)^-2$	023	14066.194	8	0
$(3,1)^-0$	103	14318.813	5	0
$(3,0)^-3$	231	15119.029	3	0

[a] Lines from previously known energy levels [17].

[b] Lines assigned to new energy levels..

Table 2: Re-assignments of $H_2{}^{16}O$ transitions from HITRAN in the 11,787 – 13,554 cm^{-1} region. I is the intensity in cm $molecule^{-1}$.

HITRAN [2]		This work					
ω (cm^{-1})	I	ω (cm^{-1})	I	Assignment			
11788.133000	2.70e-26	11788.131665	1.28e-26	211	000	4 3 1	5 5 0
11830.974000	1.33e-25	11830.974947	1.38e-25	230	000	2 1 2	1 0 1
11877.953000	6.00e-27	11877.957721	4.13e-26	230	000	6 1 6	5 0 5
11883.739000	1.90e-26	11883.743735	2.50e-26	211	000	9 2 7	10 2 8
11888.710000	1.40e-26	11888.706105	3.87e-27	230	000	7 1 7	6 0 6
11889.512000	8.08e-26	11889.509481	5.78e-26	131	000	6 2 4	6 2 5
11894.179000	3.00e-26	11894.178613	1.36e-25	310	000	9 0 9	10 1 10
11926.025000	2.50e-26	11926.028735	6.19e-26	131	000	7 4 4	7 4 3
11933.994000	1.33e-25	11933.990568	1.57e-25	131	000	7 0 7	6 0 6
11935.355600	5.54e-25	11935.355536	5.64e-25	131	000	5 4 2	5 4 1
11992.668000	3.30e-26	11992.665258	9.45e-26	310	000	6 3 4	7 2 5
11995.910600	3.12e-25	11995.910265	3.44e-25	131	000	6 2 4	5 2 3
11999.771000	1.48e-25	11999.771292	1.18e-25	032	000	6 1 6	5 2 3
12000.804500	3.94e-25	12000.804946	4.17e-25	310	000	5 0 5	6 1 6
12006.260000	1.97e-24	12006.259845	1.86e-25	131	000	8 1 7	7 1 6
12207.215000	1.10e-25	12207.214259	1.20e-25	150	000	8 6 3	7 5 2
12240.823300	4.32e-25	12240.823309	5.21e-25	211	000	7 3 5	7 1 6
12306.529000	1.08e-25	12306.531755	1.20e-25	310	000	4 2 2	3 1 3
12319.977000	2.75e-25	12319.976926	3.34e-25	310	000	5 3 3	4 2 2
12321.874000	2.88e-25	12321.875367	2.90e-25	032	000	4 4 1	3 3 0
12328.564500	8.62e-25	12328.564443	9.51e-25	310	000	6 3 4	5 2 3
12331.500200	1.72e-25	12331.499782	1.89e-25	211	000	10 3 8	9 3 7
12337.480500	7.28e-25	12337.480150	7.83e-25	310	000	8 3 6	7 2 5
12338.800500	2.75e-25	12338.801324	2.98e-25	211	000	9 2 7	8 2 6
12339.530600	1.66e-25	12339.535470	1.28e-25	211	000	8 6 2	7 6 1

12345.932000	1.78e-25	12345.932803	2.04e-25	211	000	9 4 5	8 4 4
12346.172200	3.03e-25	12346.171353	3.45e-25	211	000	9 3 6	8 3 5
12347.576000	4.02e-26	12347.571269	2.49e-26	211	000	10 4 7	9 4 6
12361.418000	1.17e-25	12361.416404	1.18e-25	211	000	10 5 5	9 5 4
12365.805000	1.44e-25	12365.802291	1.46e-25	013	000	7 2 6	8 2 7
12372.360000	2.12e-25	12372.358944	2.31e-25	131	000	6 5 1	5 3 2
12414.202700	1.47e-25	12414.203228	1.43e-25	131	000	10 7 3	9 7 2
12495.086300	2.71e-25	12495.086832	3.14e-25	112	000	6 2 5	6 1 6
12497.784000	1.16e-25	12497.785569	1.15e-25	211	000	7 3 5	6 1 6
12516.286700	6.91e-26	12516.285272	9.37e-26	112	000	7 5 2	7 4 3
12525.381600	7.12e-26	12525.386324	6.27e-26	013	000	7 5 3	7 5 2
12708.345800	1.80e-25	12708.345813	2.08e-25	112	000	6 6 1	5 5 0
12709.948500	2.62e-25	12709.949179	2.85e-25	013	000	7 3 5	6 3 4
12714.018500	2.54e-25	12714.019588	2.62e-25	013	000	7 4 4	6 4 3
12734.429400	9.42e-26	12734.426544	8.15e-26	013	000	8 4 5	7 4 4
13302.356300	1.84e-26	13302.353291	2.10e-26	240	000	4 1 4	3 0 3
13385.204100	1.23e-26	13385.206756	2.20e-26	042	000	4 1 4	4 2 3
13452.887500	7.99e-26	13452.886476	7.77e-26	320	000	7 0 7	8 1 8
13492.837000	1.27e-26	13492.834833	1.43e-26	320	000	7 0 7	7 1 6
13508.282400	1.26e-25	13508.281360	1.21e-25	221	000	8 1 7	8 3 6
13549.331600	1.11e-25	13549.330634	1.13e-25	320	000	4 2 3	5 1 4

Table 3: New assignments of $H_2{}^{16}O$ transitions listed in HITRAN in the 13,245 – 13,554 cm^{-1} region. I is the intensity in cm $molecule^{-1}$.

HITRAN [2]		This work					
ω (cm^{-1})	I	ω (cm^{-1})	I	Assignment			
13245.475400	1.55e-26			240	000	1 1 0	1 0 1
13258.920900	1.55e-26	13258.917563	1.32e-26	240	000	3 0 3	2 1 2
13264.096500	1.03e-26	13264.097585	5.35e-27	221	000	6 3 3	7 5 2

13278.471000	1.29e-26	13278.474792	9.24e-27	240	000	2 1 2	1 0 1
13299.219700	1.81e-26	13299.218993	2.07e-26	240	000	5 0 5	4 1 4
13324.777400	1.30e-26	13324.779684	5.58e-27	061	000	5 5 1	5 5 0
13338.786600	1.81e-26	13338.788140	1.80e-26	221	000	11 1 11	12 1 12
13341.880000	2.60e-26	13341.877572	2.55e-26	320	000	6 2 5	7 3 4
13347.456300	1.04e-26	13347.457352	1.14e-26	240	000	8 1 8	7 0 7
13350.988500	7.77e-27			221	000	11 2 9	12 2 10
13358.760000	1.30e-26			240	000	6 1 5	5 2 4
13370.042500	3.13e-26	13370.042059	3.42e-26	221	000	10 0 10	11 0 11
13370.857600	1.56e-26	13370.855321	1.13e-26	221	000	10 1 10	11 1 11
13371.809000	7.77e-27			240	000	2 2 1	1 1 0
13372.140500	1.04e-26	13372.137025	7.92e-27	320	000	10 2 9	11 1 10
13381.692800	1.04e-26			221	000	10 2 9	11 2 10
13384.340800	1.04e-26			221	000	10 2 8	11 2 9
13386.759900	1.56e-26	13386.762924	1.76e-26	221	000	10 1 9	11 1 10
13388.811600	1.56e-26	13388.810550	1.46e-26	240	000	7 1 6	6 2 5
13400.703600	3.92e-26	13400.702239	3.58e-26	221	000	9 0 9	10 0 10
13411.172400	4.70e-26	13411.172268	4.40e-26	221	000	9 3 7	10 3 8
13411.857200	1.57e-26	13411.854182	1.31e-26	042	000	2 1 2	2 2 1
13412.843000	1.30e-26	13412.845005	9.76e-27	320	000	5 3 2	6 4 3
13420.598000	3.40e-26	13420.594180	3.23e-26	071	000	8 0 8	9 2 7
13426.796000	1.57e-26	13426.799274	1.21e-26	301	000	9 5 4	10 5 5
13433.492300	7.81e-27	13433.495365	1.09e-26	042	000	3 1 2	3 2 1
13435.440000	1.57e-26	13435.441762	1.04e-26	122	000	7 2 5	8 5 4
13441.628900	2.62e-26	13441.626023	2.81e-26	320	000	5 2 3	6 3 4
13445.746000	1.30e-26			042	000	7 2 5	7 3 4
13446.886400	3.14e-26	13446.886192	3.01e-26	320	000	8 3 6	9 2 7
13447.408700	2.09e-26	13447.406194	2.16e-26	141	000	7 3 5	8 1 8
13459.175700	1.31e-26	13459.175365	7.53e-27	042	000	6 3 4	6 4 3

13464.176100	1.01e-25	13464.174961	8.64e-26	160	000	7 5 2	8 2 7
13464.247600	2.62e-26	13464.251845	2.69e-26	221	000	2 1 1	3 3 0
13466.500300	3.15e-26	13466.497114	2.91e-26	042	000	4 3 2	4 4 1
13467.325000	1.05e-26	13467.328865	5.86e-27	141	000	6 4 2	6 4 3
13478.288200	1.57e-26	13478.290492	7.49e-27	320	000	6 0 6	7 1 7
13482.116000	3.95e-26	13482.115641	3.77e-26	320	000	5 1 4	6 2 5
13490.611300	1.31e-26	13490.606995	7.08e-27	221	000	9 5 5	10 5 6
13493.295100	8.22e-26	13493.296899	8.22e-26	240	000	6 4 3	7 1 6
13494.968000	2.46e-25	13494.967605	2.68e-25	301	000	6 1 5	7 3 4
13498.145700	1.57e-26	13498.146661	3.57e-27	320	000	4 1 3	5 2 4
13502.174100	6.09e-26	13502.174835	5.74e-26	400	000	9 2 7	10 3 8
13503.662300	2.89e-26	13503.660893	2.41e-26	320	000	5 0 5	6 1 6
13505.400700	1.57e-26	13505.400612	2.80e-26	320	000	8 4 5	9 3 6
13505.925100	5.27e-26			400	000	10 1 9	11 2 10
13508.679900	3.69e-26	13508.682770	2.56e-26	061	000	10 5 5	11 1 10
13510.874100	1.31e-26	13510.875169	7.20e-27	141	000	6 4 3	7 2 6
13512.802000	1.31e-26	13512.803426	1.13e-26	141	000	4 4 0	5 2 3
13514.615200	2.11e-26	13514.615247	1.92e-26	320	000	3 1 2	4 2 3
13515.340700	1.84e-26	13515.343063	1.04e-26	400	000	7 6 1	7 7 0
13518.004500	4.74e-26	13518.004076	4.28e-26	320	000	5 2 4	6 1 5
13522.418200	4.21e-26			221	000	8 5 3	9 5 4
13522.460600	4.50e-26			320	000	6 3 4	7 2 5
13525.932800	4.50e-26	13525.935724	2.78e-26	400	000	4 4 1	5 5 0
13526.091700	1.84e-26	13526.094044	3.68e-27	320	000	8 3 6	8 4 5
13526.575700	1.84e-26			320	000	4 0 4	5 1 5
13528.596300	3.16e-26	13528.596797	1.83e-26	240	000	4 3 1	3 2 2
13528.718100	3.43e-26	13528.714004	2.20e-26	400	000	5 1 5	6 2 4
13530.770000	2.64e-26	13530.774475	1.77e-26	042	000	7 5 2	7 6 1
13536.064500	1.05e-26			400	000	9 4 6	10 3 7

13537.532900	1.84e-26	13537.528149	1.07e-26	160	000	9 8 1	9 9 0
13539.255000	2.11e-26	13539.254278	1.05e-26	221	000	1 0 1	2 2 0
13540.914600	3.43e-26	13540.914252	2.18e-26	320	000	6 5 2	6 6 1
13541.763800	6.09e-26	13541.765461	4.59e-26	042	000	9 3 6	10 2 9
13547.017300	3.17e-26	13547.014951	4.16e-26	320	000	3 0 3	4 1 4
13548.022200	3.17e-26	13548.025843	3.74e-26	320	000	7 4 4	8 3 5
13548.150100	2.90e-26	13548.150470	2.20e-26	320	000	6 3 4	6 4 3
13549.083900	1.32e-26	13549.080652	8.24e-27	141	000	8 5 3	8 5 4
13550.134100	3.70e-26	13550.132062	2.95e-26	400	000	7 1 6	7 4 3